Optics and Lasers in Engineering ▮ (▮▮▮▮) ▮▮▮–▮▮▮

Contents lists available at ScienceDirect

Optics and Lasers in Engineering

journal homepage: www.elsevier.com/locate/optlaseng

Measurement of edge residual stresses in glass by the phase-shifting method

A. Ajovalasit *, G. Petrucci, M. Scafidi

Dipartimento di Meccanica, University of Palermo, viale delle Scienze, 90128 Palermo, Italy

ARTICLE INFO

Article history:
Received 6 September 2010
Received in revised form
13 December 2010
Accepted 4 January 2011

Keywords:
Residual stresses
Glass
Photoelasticity
Phase shifting
Image processing

ABSTRACT

Control and measurement of residual stress in glass is of great importance in the industrial field. Since glass is a birefringent material, the residual stress analysis is based mainly on the photoelastic method. This paper considers two methods of automated analysis of membrane residual stress in glass sheets, based on the phase-shifting concept in monochromatic light. In particular these methods are the automated versions of goniometric compensation methods of Tardy and Sénarmont. The proposed methods can effectively replace manual methods of compensation (goniometric compensation of Tardy and Sénarmont, Babinet and Babinet–Soleil compensators) provided by current standards on the analysis of residual stresses in glasses.

1. Introduction

It is known that photoelasticity can be used for residual stress analysis in glass sheets [1–3]. These stresses are usually identified as *thickness stresses* (variable in depth) and *membrane stresses* (constant in depth), which are the subject of this paper. The two-dimensional photoelastic analysis of membrane residual stresses and, in particular, of the edge stresses has been the subject of several contributions, technical standards and commercial equipment based on the use of Babinet and Babinet–Soleil compensators [4–6], Sénarmont compensation [7,8], SCA—Spectral content Analysis [6,9] and the Grey Field Polariscope [10,11].

In this paper phase-shifting photoelasticity [12–14] is applied for the determination of membrane residual stresses at the edge of glass sheets. Since the isoclinic parameter is known at the boundary, two simplified phase-shifting methods are used: the first, initially proposed by Asundi [15], is based on the set-up of the Tardy compensation (briefly called *Tardy Phase Shifting*), the second one, developed in this paper, is based on the Sénarmont compensation set-up (briefly called *Sénarmont Phase Shifting*). Besides the theoretical formulation of the proposed methods, the influences of isoclinic error and of the quarter-wave plates' error on the determination of the retardation are considered for both methods. Finally, the theory has been experimentally validated by comparing the results obtained by the proposed methods with those provided by the goniometric compensation methods of Tardy and Sénarmont.

2. Theoretical analysis

In general, the phase-shifting methods are based on the acquisition of at least four images (more frequently six), obtained usually by rotating both the analyser and its quarter-wave plate [12–14].

The simplified phase-shifting methods used in this research have the same limitation of the goniometric compensation methods of Tardy and Sénarmont, i.e. the prior knowledge of the directions of principal stresses. Nevertheless, the directions of principal stress are always known at the boundaries (tangent and normal), and hence the preference for the simplified methods. In addition, these methods have the following advantages: (a) only three acquisitions are necessary, (b) the formula for the determination of retardation does not contain the isoclinic parameter and (c) the rotation of the analyser quarter-wave plate is not required, as it occurs in the general methods of phase shifting.

In the Tardy phase-shifting method the model is initially placed in a dark field circular polariscope (Fig. 1a). If the analyser is rotated by an angle β_A (Fig. 1b), using the Jones matrix calculus [16] the light intensity emerging from the analyser can be written as

$$I = I_f + \frac{I_0}{2}(1 - \cos 2\pi\delta \cos 2\beta_A + \sin 2\pi\delta \sin 2\beta_A \cos 2\alpha) \quad (1)$$

where I_f and I_0 are the background intensity and the fringe intensity term, respectively, α is the angle between the maximum principal stress σ_1 and the horizontal reference axis (Fig. 1b) and δ is the

* Corresponding author. Tel.: +39 091 6657 135; fax: +39 091 484 334.
E-mail addresses: ajovalasit@dima.unipa.it (A. Ajovalasit), petrucci@dima.unipa.it (G. Petrucci), scafidi@dima.unipa.it (M. Scafidi).

0143-8166/$ - see front matter © 2011 Elsevier Ltd. All rights reserved.
doi:10.1016/j.optlaseng.2011.01.004

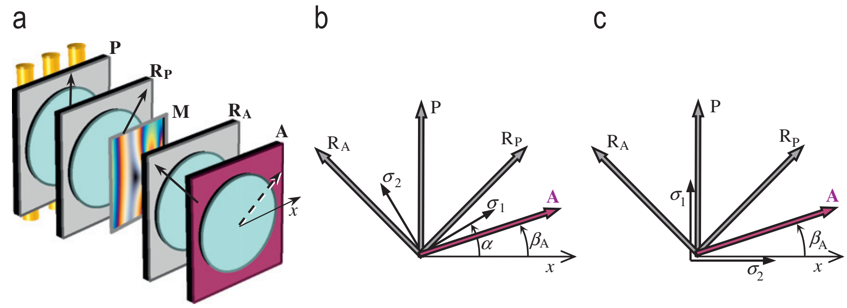

Fig. 1. (a) Set-up of the polariscope for Tardy compensation and for the Tardy phase-shifting method, (b) general orientation of principal stresses and (c) vertical maximum principal stress (aligned with the polariser).

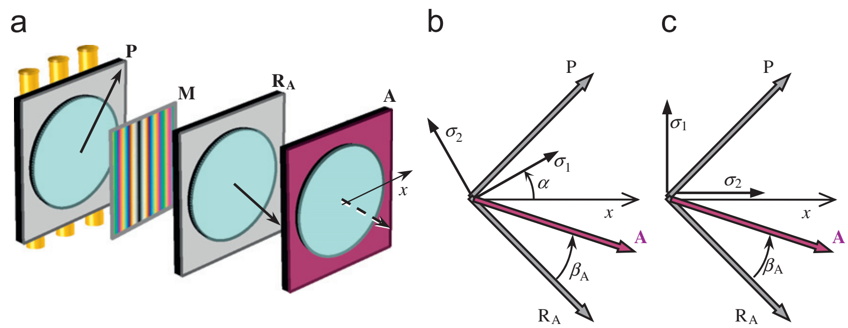

Fig. 2. (a) Set-up of the polariscope for Sénarmont compensation and for the Sénarmont phase-shifting method, (b) general orientation of principal stresses and (c) vertical maximum principal stress.

retardation that is linked to the principal stresses σ_1 and σ_2 by the well known equation:

$$\delta=\frac{Cd}{\lambda}(\sigma_1-\sigma_2) \tag{2}$$

where C is the photoelastic constant of the glass, d is the glass thickness and λ is the wavelength of the monochromatic light source.

Similarly, in the Sénarmont phase-shifting method the model is initially placed in a dark field plane polariscope arranged for the Sénarmont compensation (Fig. 2a) with the polariser P oriented at $+45^\circ$, the analyser A and its quarter-wave plate R_A oriented at -45°. If the analyser is rotated by an angle β_A with respect to the initial position aligned with the quarter-wave plate (Fig. 2b), the light intensity emerging from the analyser is

$$I=I_f+\frac{I_0}{2}\left[1+\sin 2\pi\delta\cos 2\alpha\sin 2\beta_A - (\cos^2 2\alpha\cos 2\pi\delta+\sin^2 2\alpha)\cos 2\beta_A\right] \tag{3}$$

Now the points of the model where the principal stresses are directed along the axes x and y (horizontal and vertical) are considered: to achieve this condition at the boundary is sufficient to have the glass sheet with the boundary parallel or perpendicular to the x horizontal axis. In particular, assuming the maximum principal stress directed along the vertical y-axis ($\alpha=90^\circ$, Figs. 1c and 2c) the light intensity emerging from the analyser is from both Eqs. (1) and (3):

$$I_i=I_f+\frac{I_0}{2}\left[1-\cos(2\pi\delta-2\beta_{Ai})\right],\quad (i=1,2,3\ldots) \tag{4}$$

Eq. (4), valid for both Tardy and Sénarmont phase-shifting methods, shows that there are three unknowns, i.e. I_f, I_0 and δ, even if the unknown of interest is only the retardation δ, and therefore at least three images, obtained by rotating only the analyser, have to be acquired.

In particular, the methods for the determination of δ described below are based on four acquisitions (I_1, I_2, I_3 and I_4) made by angles $\beta_{A1}=0^\circ$, $\beta_{A2}=45^\circ$, $\beta_{A3}=90^\circ$ and $\beta_{A4}=135^\circ$ $(=-45^\circ)$ and on three acquisitions (only I_1, I_2 and I_3). The light intensities corresponding to the four above-mentioned values of β_A are for both the Tardy and Sénarmont phase-shifting methods:

$$I_1=I_f+\frac{I_0}{2}(1-\cos 2\pi\delta) \tag{5}$$

$$I_2=I_f+\frac{I_0}{2}(1-\sin 2\pi\delta) \tag{6}$$

$$I_3=I_f+\frac{I_0}{2}(1+\cos 2\pi\delta) \tag{7}$$

$$I_4=I_f+\frac{I_0}{2}(1+\sin 2\pi\delta) \tag{8}$$

Eqs. (5)–(8) allow us to obtain the retardation δ as

$$\tan 2\pi\delta=\frac{I_4-I_2}{I_3-I_1} \tag{9}$$

Alternatively, using just the first three acquisitions (5)–(7), the retardation can be obtained as

$$\tan 2\pi\delta=\frac{I_1+I_3-2I_2}{I_3-I_1} \tag{10}$$

However, due to the periodicity of the tangent function, Eqs. (9) and (10) provide only the fractional retardation δ_f, which is defined in the range ± 0.5 fringe orders. In order to determine the total retardation δ, well known unwrapping procedures are used, provided that the user specifies the fringe order at one point.

Eq. (2) allows us to determine the difference of the principal stresses, provided that the retardation δ and the photoelastic constant C are known from the measurements. Particularly at the edges (usually compressed, i.e. $\sigma_1=0$) Eq. (2) provides:

$$\sigma_2 = -\frac{\lambda}{Cd}\delta \tag{11}$$

To determine the photoelastic constant C (for glass $C=-2$–5 Brewster $(=\mathrm{TPa}^{-1})$) of the glass under investigation, well known calibration methods, also provided by a specific technical standard on glass [17], are used.

2.1. Influence of the isoclinic parameter and of the quarter-wave plates errors

If the contour of the glass is straight and correctly positioned, then the isoclinic parameter is correct near the boundary ($\alpha=90°$). At some distance, the isoclinic parameter can be affected by an error, usually negligible because the analysis is limited to a small depth (about 20 mm) near the boundary itself. If the edge is curved, even at the boundary the isoclinic parameter is affected by an error with respect to the ideal value $\alpha=90°$. In general, then, the isoclinic parameter is affected by an error ε_i respect to the ideal value $\alpha=90°$, i.e.

$$\alpha = 90° + \varepsilon_i \tag{12}$$

In addition, the quarter-wave plates may have a retardation that is affected by an error ε respect to the ideal value $\gamma=90°$, i.e.

$$\gamma = 90° + \varepsilon \tag{13}$$

In the presence of the errors mentioned above, the retardation calculated through Eqs. (9) and (10) provides incorrect values. The effect of the isoclinic error (ε_i) on the retardation obtained by the Tardy (δ_T') and the Sénarmont phase-shifting methods (δ_S') is given by the following equations (see Appendix):

$$\tan 2\pi\delta_T' = \frac{I_4'-I_2'}{I_3'-I_1'} = \tan 2\pi\delta \cos 2\varepsilon_i \tag{14}$$

$$\tan 2\pi\delta_S' = \frac{I_4'-I_2'}{I_3'-I_1'} = \frac{\sin 2\pi\delta \cos 2\varepsilon_i}{\cos 2\pi\delta \cos^2 2\varepsilon_i + \sin^2 2\varepsilon_i} \tag{15}$$

The effect of the quarter-wave plates error (ε) on the retardation obtained by the Tardy (δ_T') and the Sénarmont phase-shifting methods (δ_S') is as follows (see Appendix):

$$\tan 2\pi\delta_T' = \frac{I_4'-I_2'}{I_3'-I_1'} = \frac{\sin 2\pi\delta \cos \varepsilon}{\cos 2\pi\delta \cos^2 \varepsilon + \sin^2 \varepsilon} \tag{16}$$

$$\tan 2\pi\delta_S' = \frac{I_4'-I_2'}{I_3'-I_1'} = \tan 2\pi\delta \cos \varepsilon \tag{17}$$

The correspondence between Eqs. (14) and (17) and between Eqs. (15) and (16) considering $\varepsilon=2\varepsilon_i$ should be noted. Eqs. (14)–(17) coincide with those obtained for the goniometric compensation methods of Tardy and Sénarmont [18,19]. Consequently, the following well known considerations are valid:

1. if the isoclinic parameter is correct ($\varepsilon_i=0$) and the quarter-wave plates are not correct ($\varepsilon \neq 0$), the Sénarmont method is more accurate than the Tardy method [18];
2. if the isoclinic parameter is not correct ($\varepsilon_i \neq 0$) and the quarter-wave plates are correct ($\varepsilon=0$), the Sénarmont method is less accurate than the Tardy method [19].

For the general case of simultaneous presence of errors ε_i and ε, reference is made to the bibliography on the goniometric compensation methods [20].

Fig. 3 considers the effect of the isoclinic error alone. In particular Fig. 3a shows the error $\delta'-\delta$ as a function of the retardation δ variable in the range 0–1 fringe orders for an isoclinic error $\varepsilon_i=10°$; Fig. 3b shows the maximum absolute error $|\delta'-\delta|$ as a function of the isoclinic error ε_i. The figure confirms that, as for the methods of goniometric compensation (Tardy and Sénarmont), the isoclinic error is not critical. The theoretical results obtained here confirm the experimental observation of Asundi [15] about the limited influence of the incorrect positioning of the isoclinics on the Tardy phase-shifting method. It should be noted that, owing to the correspondence between Eqs. (14) and (17) and between Eqs. (15) and (16), Fig. 3b can be used to estimate the error due to the quarter-wave plates' error: to do this, simply reverse the Tardy curve with the Sénarmont one and consider, on the horizontal axis, $\varepsilon_i=\varepsilon/2$.

3. Experiments

The acquisition system used in these experiments is composed of:

1. a polariscope with a monochromatic light source provided by yellow sodium vapour lamps ($\lambda=589$ nm) with quarter-wave plates correct for that yellow light (with error ε less than 6°);

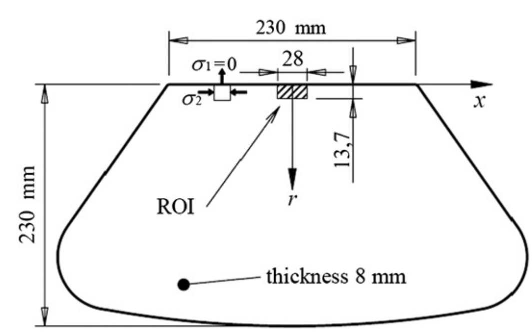

Fig. 4. Shelf in tempered glass used for the experiments and Region Of Interest (ROI).

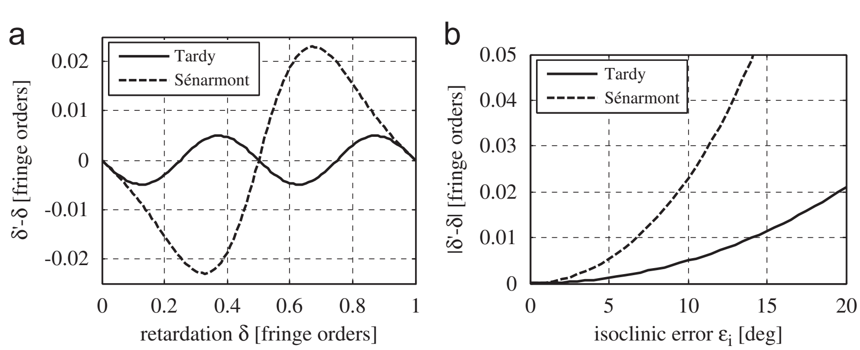

Fig. 3. Error due to the isoclinic error alone: (a) error as a function of the retardation δ for $\varepsilon_i=10°$ and (b) maximum absolute error as a function of the isoclinic error ε_i.

Please cite this article as: Ajovalasit A, et al. Measurement of edge residual stresses in glass by the phase-shifting method. Opt Laser Eng (2011), doi:10.1016/j.optlaseng.2011.01.004

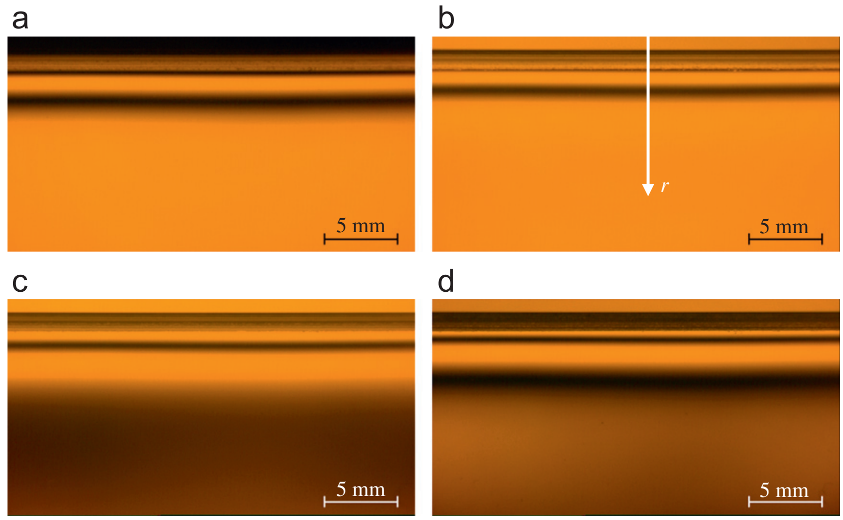

Fig. 5. ROI images obtained by the Tardy phase-shifting method in monochromatic yellow light. (The images were acquired with the following angles of the analyser: 0° (a), 45° (b), 90° (c) and 135° (d)).

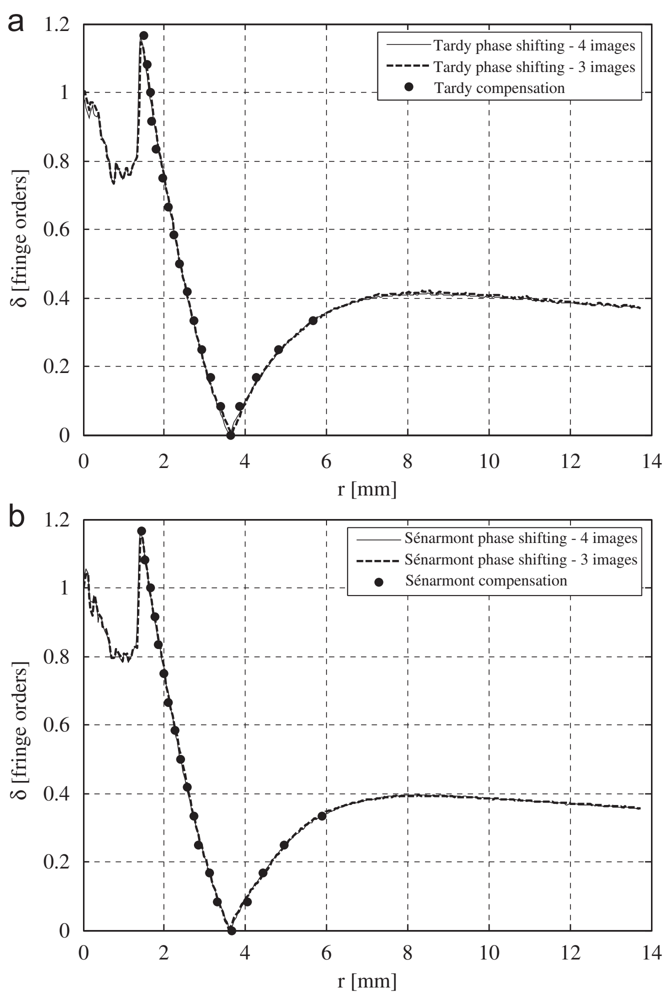

Fig. 6. Retardation δ along the direction r normal to the contour of the glass: (a) Tardy phase-shifting method and (b) Sénarmont phase-shifting method.

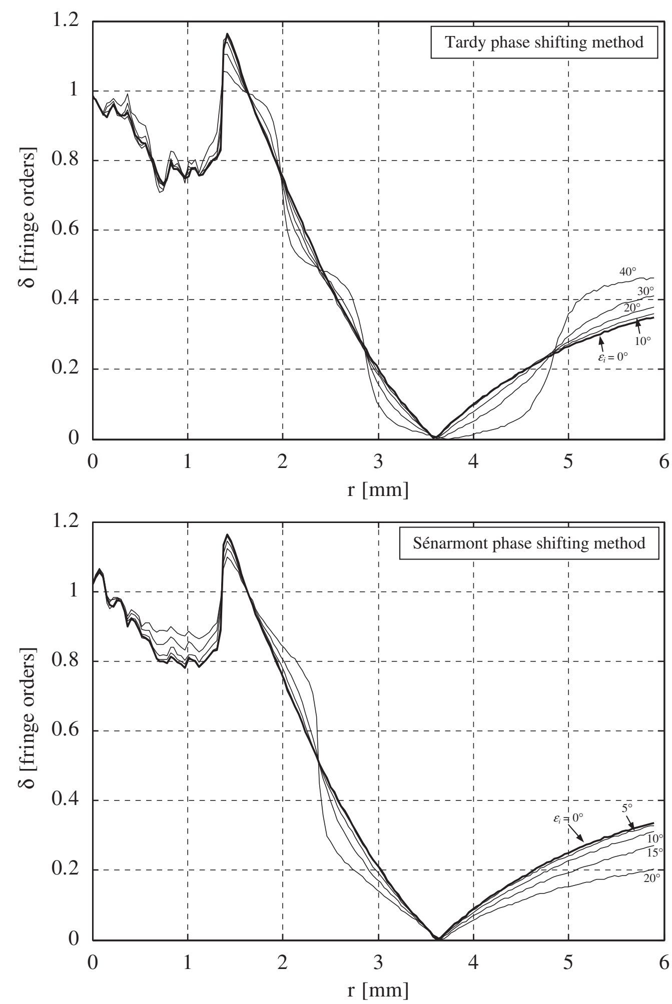

Fig. 7. Retardation δ along the direction r normal to the contour of the glass when the glass sheet is rotated: (top) Tardy phase-shifting method and (bottom) Sénarmont phase-shifting method.

2. an RGB camera with three independent CCD sensors, model JVC KY-F30 with a resolution of 768×576 pixels;
3. a 24 bit analogue–digital converter (digitizer);
4. a personal computer.

The experiments were performed on a household shelf in tempered glass with thickness $d = 8$ mm (Fig. 4). In order to realise the condition for alignment of the principal stresses that the theory of the proposed methods requires (Figs. 1c and 2c), the upper edge of the glass sheet has been aligned with the horizontal x-axis direction.

For each method, four acquisitions of the Region Of Interest (ROI) (Fig. 4), corresponding to $\beta_{A1}=0^\circ$, $\beta_{A2}=45^\circ$, $\beta_{A3}=90^\circ$ and $\beta_{A4}=135^\circ$ $(=-45^\circ)$ were carried out. As an example, Fig. 5 shows the four images of the ROI for the Tardy phase-shifting method.

Moreover, to highlight the effect of incorrect isoclinic angle further acquisitions were made by rotating the glass in its plane in order to introduce known errors ε_i on the isoclinic parameter at the boundary. The error due to quarter-wave plates was not considered as, for $\varepsilon=6^\circ$, the error on the retardation is negligible (around 0.002 and 0.0004 fringe orders for Tardy and Sénarmont methods, respectively).

Fig. 6 shows the results obtained with the proposed methods (Tardy and Sénarmont phase-shifting methods) using both three and four image methods, in the case of correctly positioned contour. It should be noted that methods based on the use of three and four images provide, in practise, the same results; therefore, methods based on the use of only three images can be considered satisfactory. The irregularity of the retardation near the edge (r close to 0) is due to the bevelled region of the glass. As in the manual methods, the retardation must be extrapolated at the boundary according to well known procedures [4,5] (the extrapolation is not shown in the figure). For comparison the results with the manual methods (Tardy and Sénarmont compensation) are shown. The precision of the results obtained by the automated methods is equivalent to that of the manual methods, while the automated methods allow a significant reduction in the number of acquisitions (from approximately 20 to only 3) and allow the full field determination of the retardation δ in the ROI.

Fig. 7 shows, in addition to the results of Fig. 6, the results obtained introducing rotations of the boundary of the glass by angles of 10°, 20°, 30° and 40° for the Tardy method and of 5°, 10°, 15° and 20° for the Sénarmont method. It should be noted that the errors are consistent with those given by the Eqs. (14) and (15) and with those shown in Fig. 3a. In particular, the errors of the Tardy method are lower and become null for values of the retardations of 0, 0.25, 0.5, 0.75, 1, etc. fringe orders, while the errors of the Sénarmont method vanish only for retardations of 0, 0.5, 1, etc. fringe orders. In both methods the position of the contour is not critical: the error is lower than 0.025 fringe orders for an isoclinic error of 20° and 10° for the Tardy method and the Sénarmont method, respectively.

4. Discussion

In short, the experiments show that:

1. results obtained by phase-shifting methods and goniometric compensation methods are in good agreement, with significant advantages of the automated methods concerning: (a) the required number of acquisitions (from about 20 for the goniometric compensation methods to only 3 for the phase-shifting methods), (b) the full field determination of the retardation δ in the ROI;
2. the phase-shifting methods proposed in this paper require prior knowledge of the orientation of the principal stresses, as goniometric methods (Tardy and Sénarmont); they are, however, easily applicable, because the ROI is near the edge of the glass;
3. in the case of quarter-wave plates without error, the Tardy phase-shifting method is more precise than the Sénarmont phase-shifting method; however, the positioning of the glass boundary is not critical, because the allowed error on the isoclinic parameter is approximately about 10° and 20° for Sénarmont and Tardy methods, respectively; in the case of large variations of the isoclinic parameter, the general phase-shifting methods can be used [12–14].

5. Conclusions

This research describes the theory and the application of two phase-shifting methods to the determination of membrane residual stresses at the edge of a glass sheet. The proposed methods are based on the polariscope set-ups used for the Tardy and Sénarmont goniometric compensation.

These phase-shifting methods allow the full field determination of the retardation, and therefore of the stress, at the edges of the glass, using only three acquisitions in monochromatic light. The results are in good agreement with those obtained by the manual techniques of Tardy and Sénarmont compensation. The restrictions of the proposed techniques are the same as those of the above cited compensation methods, as the errors due to incorrect isoclinic setting and quarter-wave plates error are the same for the proposed techniques and the corresponding compensation methods. The number of acquisitions decreases significantly from about 20 to just 3 acquisitions and results are obtained in full field.

Thus, digital photoelasticity enables the automation of manual methods of compensation currently provided in the technical standards concerning the analysis of membrane residual stresses in glasses.

Appendix

A.1. Tardy phase-shifting method

A.1.1. Effect of the isoclinic error ε_i [Eq. (14)]

In the presence of an isoclinic error ε_i (see Eq. (12)), Eq. (1) becomes:

$$I' = I_f + \frac{I_0}{2}(1-\cos 2\pi\delta \cos 2\beta_A - \sin 2\pi\delta \sin 2\beta_A \cos 2\varepsilon_i) \tag{A1}$$

Under these conditions the light intensities I_1, I_2 I_3 and I_4, given by Eqs. (5)–(8) become:

$$I'_1 = I_1 = I_f + \frac{I_0}{2}(1-\cos 2\pi\delta) \tag{A2}$$

$$I'_2 = I_2 = I_f + \frac{I_0}{2}(1-\sin 2\pi\delta \cos 2\varepsilon_i) \tag{A3}$$

$$I'_3 = I_3 = I_f + \frac{I_0}{2}(1+\cos 2\pi\delta) \tag{A4}$$

$$I'_4 = I_4 = I_f + \frac{I_0}{2}(1+\sin 2\pi\delta \cos 2\varepsilon_i) \tag{A5}$$

The light intensities of the first and third images (Eqs. (A2) and (A4)) are not affected by isoclinic error since these images are acquired with the circular polariscope in dark field and bright field.

Eqs. (A2)–(A5) give:

$$\tan 2\pi\delta'_T = \frac{I'_4 - I'_2}{I'_3 - I'_1} = \tan 2\pi\delta \cos 2\varepsilon_i \tag{A6}$$

which coincides with Eq. (14); the same result is obtained using only the first three acquisitions.

A.1.2. Effect of quarter-wave plates error ε (Eq. (16))

In the presence of an error ε of the quarter-wave plates, the light intensities I_1, I_2, I_3 and I_4, given by Eqs. (5)–(8) become:

$$I'_1 = I_1 = I_f + \frac{I_0}{2}(1-\cos 2\pi\delta)\cos^2\varepsilon \tag{A7}$$

$$I'_2 = I_2 = I_f + \frac{I_0}{2}(1-\sin 2\pi\delta \cos 2\varepsilon) \tag{A8}$$

$$I'_3 = I_3 = I_f + \frac{I_0}{2}\left[2\sin^2\varepsilon + (1+\cos 2\pi\delta)\cos^2\varepsilon\right] \tag{A9}$$

$$I'_4 = I_4 = I_f + \frac{I_0}{2}(1+\sin 2\pi\delta\cos 2\varepsilon) \tag{A10}$$

Eqs. (A7)–(A10) give:

$$\tan 2\pi\delta'_T = \frac{I'_4 - I'_2}{I'_3 - I'_1} = \frac{\sin 2\pi\delta\cos\varepsilon}{\cos 2\pi\delta\cos^2\varepsilon + \sin^2\varepsilon} \tag{A11}$$

which coincides with Eq. (16); the same result is obtained using only the first three acquisitions.

A.2. Sénarmont phase-shifting method

A.2.1. effect of the isoclinic error ε_i (Eq. (15))

In the presence of an isoclinic error ε_i (see Eq. (12)), Eq. (3) becomes:

$$I = I_f + \frac{I_0}{2}[1 - \sin 2\pi\delta\cos 2\varepsilon_i \sin 2\beta_A] \\ -(\cos^2 2\varepsilon_i \cos 2\pi\delta + \sin^2 2\varepsilon_i)\cos 2\beta_A] \tag{A12}$$

Under these conditions the light intensities I_1, I_2, I_3 and I_4, given by Eqs.(5)–(8) become:

$$I'_1 = I_f + \frac{I_0}{2}(1-\cos 2\pi\delta)\cos^2 2\varepsilon_i \tag{A13}$$

$$I'_2 = I_f + \frac{I_0}{2}(1-\sin 2\pi\delta\cos 2\varepsilon_i) \tag{A14}$$

$$I'_3 = I_f + \frac{I_0}{2}\left[2\sin^2 2\varepsilon_i + (1+\cos 2\pi\delta)\cos^2 2\varepsilon_i\right] \tag{A15}$$

$$I'_4 = I_f + \frac{I_0}{2}(1+\sin 2\pi\delta\cos 2\varepsilon_i) \tag{A16}$$

Eqs. (A13)–(A16) give:

$$\tan 2\pi\delta'_S = \frac{I'_4 - I'_2}{I'_3 - I'_1} = \frac{\sin 2\pi\delta\cos 2\varepsilon_i}{\cos 2\pi\delta\cos^2 2\varepsilon_i + \sin^2 2\varepsilon_i} \tag{A17}$$

which coincides with Eq. (15); the same result is obtained using only the first three acquisitions.

A.2.2. Effect of quarter-wave plates error ε (Eq. (17))

In the presence of an error ε of the quarter-wave plates, the light intensities I_1, I_2, I_3 and I_4, given by Eqs. (5)–(8) become:

$$I'_1 = I_f + \frac{I_0}{2}(1-\cos 2\pi\delta) \tag{A18}$$

$$I'_2 = I_f + \frac{I_0}{2}(1-\sin 2\pi\delta\cos\varepsilon) \tag{A19}$$

$$I'_3 = I_f + \frac{I_0}{2}(1+\cos 2\pi\delta) \tag{A20}$$

$$I'_4 = I_f + \frac{I_0}{2}(1+\sin 2\pi\delta\cos 2\varepsilon) \tag{A21}$$

The light intensities of the first and third image (Eqs. (A18) and (A20)) are not affected by isoclinic error since these images are acquired with the plane polariscope in dark field and bright field.

Eqs. (A18)–(A21) give:

$$\tan 2\pi\delta'_S = \frac{I'_4 - I'_2}{I'_3 - I'_1} = \tan 2\pi\delta\cos\varepsilon \tag{A22}$$

which coincides with Eq. (17); the same result is obtained using only the first three acquisitions.

References

[1] Aben H, Guillemet C. Photoelasticity of Glass. Berlin: Springer; 1993.
[2] McKenzie HW, Hand RJ. Basic Optical Stress Measurement in Glass. Sheffield: Society of Glass Technology; 1999.
[3] Aben H, Anton J, Errapart A. Modern photoelasticity for residual stress measurement in glass. Strain 2008;44:40–8.
[4] Redner AS, Voloshin AS. Surface and face stress in tempered glass. In: Proceedings of 9th international conference on experimental mechanics. vol. 2, Copenhagen; 1990, p. 884–91.
[5] ASTM 1279. Standard test method for non-destructive photoelastic measurement of edge and surface stresses in annealed, heat-strengthened, and fully tempered flat glass. Annual Book of ASTM Standards. ASTM, West Conshohocken, PA, USA.
[6] Strainoptic Inc. Glass Application & Plastic Application. Available at 〈http://www.strainoptic.com〉, 2010.
[7] ASTM F218. Standard method for analyzing stress in glass. Annual Book of ASTM Standards. ASTM, West Conshohocken, PA, USA.
[8] Sharples Stress Engineers Ltd. Strain Viewer. Available at 〈http://www.sharplesstress.com〉, 2010.
[9] Redner AS. Automated measurement of edge stress in automotive glass. In: Proceedings of the conference on glass processing days. Tampere, Finland; 2003, p. 578–99.
[10] Zickel MJ, Lesniak JR, Tate DJ, La Brecque R, Harkins K. Residual stress measurement of auto windshields using the Grey Field Polariscope. Spring '99 SEM Conference. Cincinnati, OH, USA; 1999.
[11] Stress Photonics, Inc. Glass inspection products. Available at 〈http://www.glassphotonics.com〉, 2010.
[12] Ajovalasit A, Barone S, Petrucci G. A review of automated methods for the collection and analysis of photoelastic data. Journal of Strain Analysis 1998;33(29):75–91.
[13] Ramesh K. Digital Photoelasticity. Berlin: Springer; 2000.
[14] Patterson EA. Digital photoelasticity: principles, practice and potential. Strain 2002;38(1):27–39.
[15] Asundi A. Phase shifting in photoelasticity. Experimental Techniques 1993:19–23.
[16] Theocaris PS, Gdoutos EE. Matrix Theory of Photoelasticity. Berlin: Springer; 1979.
[17] ASTM C978. Standard test method for photoelastic determination of residual stress in a transparent glass matrix using a polarizing microscope and optical retardation compensation procedures. Annual Book of ASTM Standards. ASTM, West Conshohocken, PA, USA.
[18] Jessop HT. On the Tardy and Sénarmont methods of measuring fractional relative retardations. British Journal of Applied Physics 1953;4(5):138–41.
[19] Chakrabarti SK, Machin KE. Accuracy of compensation methods in photoelastic fringe-order measurements. Experimental Mechanics 1969;9(8):429–31.
[20] Sathiks SM, Bigg GW. On the accuracy of goniometric compensation methods in photoelastic fringe order measurements. Experimental Mechanics 1972;12(1):47–9.

Please cite this article as: Ajovalasit A, et al. Measurement of edge residual stresses in glass by the phase-shifting method. Opt Laser Eng (2011), doi:10.1016/j.optlaseng.2011.01.004